LETTER

Astron. Astrophys. 335, L106–L110 (1998)

ASTRONOMY AND ASTROPHYSICS

*Letter to the Editor*

# VLBI observations of the galactic center source Sgr A* at 86 GHz and 215 GHz

**T.P. Krichbaum[1], D.A. Graham[1], A. Witzel[1], A. Greve[2], J.E. Wink[2], M. Grewing[2], F. Colomer[3], P. de Vicente[3], J. Gómez–González[3], A. Baudry[4], and J.A. Zensus[1]**

[1] Max-Planck-Institut für Radioastronomie, Auf dem Hügel 69, D-53121 Bonn, Germany
[2] Institut de Radioastronomie Millimétrique, F-38406 St. Martin d'Hères, France
[3] Centro Astronómico de Yebes, Apartado 148, E-19080 Guadalajara, Spain
[4] Observatoire de Bordeaux, B.P. 89, F-33270 Floirac, France

Received 17 April 1998 / Accepted 8 May 1998

**Abstract.** We have observed and detected Sgr A* with VLBI at 86 GHz and at 215 GHz in March 1995. At 86 GHz the measured closure phase is close to zero, consistent with a point-like or symmetric structure of $190\pm30$ $\mu$as in size. At 215 GHz we have detected Sgr A* with a signal-to-noise ratio of 6. This yields a tentative size estimate of $110 \pm 60$ $\mu$as which, despite of a limited calibration accuracy and uncertainty in the origin of the mm/sub-mm total flux density excess, lies well above the scattering size of $20\mu$as at this frequency. The intrinsic size of Sgr A* thus appears to be $17 \pm 9$ Schwarzschild radii for a $2.6 \cdot 10^6$ $M_\odot$ black hole.

**Key words:** Galaxy: center – galaxies: individual: Sgr A* – scattering – techniques: interferometry – galaxies: nuclei

## 1. Introduction

Observations of the compact radio source Sgr A* and the motions of stars in its vicinity yield strong evidence for a massive black hole of $\sim 2.6\cdot10^6$ $M_\odot$ in the center of our Galaxy (Genzel et al. 1997, see also Mezger et al. 1996 and references therein). At short millimeter wavelengths, VLBI observations carry the potential to image Sgr A* with a spatial resolution of only a few Schwarzschild radii ($R_s$) (at a distance of 8 kpc, 1 $R_s$ corresponds to an angle of $\sim 6.5\mu$as). At cm-wavelengths the VLBI image of Sgr A* appears broadened by diffractive scattering from ionized material surrounding the Galactic Center region. The scattering size decreases quadratically with frequency and approaches the intrinsic source size (defined by $R_s$) at short mm-wavelengths. Millimeter VLBI observations therefore should allow to image directly the intrinsic source structure free from scattering.

Recent VLBI observations at 43 GHz (Krichbaum et al. 1993, Backer et al. 1993, Bower et al. 1997, hereafter B97) and 86 GHz (Rogers et al. 1994, Krichbaum et al. 1994) are consistent with a point-like–or perhaps slightly east-west elongated structure–with a size close to the expected scattering size. More observations at short millimeter wavelengths ($\lambda \leq 3.5$ mm) are necessary to investigate up to which frequency the image of Sgr A* is scatter broadened.

In this paper, we present results from VLBI observations at 86 GHz (3.5 mm) and 215 GHz (1.4 mm). At 86 GHz, we were for the first time able to measure the structure closure phase of Sgr A*. At 215 GHz, Sgr A* was detected on the 1150 km baseline between Pico Veleta and Plateau de Bure. This observation provides a first size estimate at 1.4 mm wavelength.

## 2. Observations

We observed Sgr A* in two millimeter-VLBI experiments in March 1995 at 86 GHz with the 100 m antenna of the MPIfR at Effelsberg (Germany) (B), the IRAM 30 m antenna at Pico Veleta (Spain) (X), and one 15 m antenna of the IRAM interferometer at Plateau de Bure (France) (P). At 215 GHz, Pico Veleta and Plateau de Bure participated in the observation.

At 86 GHz, useful data of Sgr A* were obtained during the period March 8, 04h15–09h30 UT. At 215 GHz, the data cover the period 0h00–08h00 UT on March 2. The experimental setup, the data recording (MK III, mode A, 112 MHz bandwidth, 6.5 min scans every 15 min), and the calibration strategy in both experiments were similar and are described in detail by Greve et al., 1995 (hereafter G95) and Krichbaum et al., 1997 (hereafter K97). The data were correlated in Bonn and fringe fitted and calibrated using the standard correlator software, the Caltech VLBI package, Difmap, and AIPS (for details see K97). To improve the calibration (based on measurements of $T_{\rm sys}$ and antenna gains) we observed as calibrators at 86 GHz and 215 GHz the source NRAO 530, and at 86 GHz the SiO maser VX Sgr. NRAO 530 was observed in 6.5 min scans alternating with observations of Sgr A*. VX Sgr was observed in 60 sec scans before each Sgr A* scan (of 330 sec duration).

*Send offprint requests to*: T.P. Krichbaum

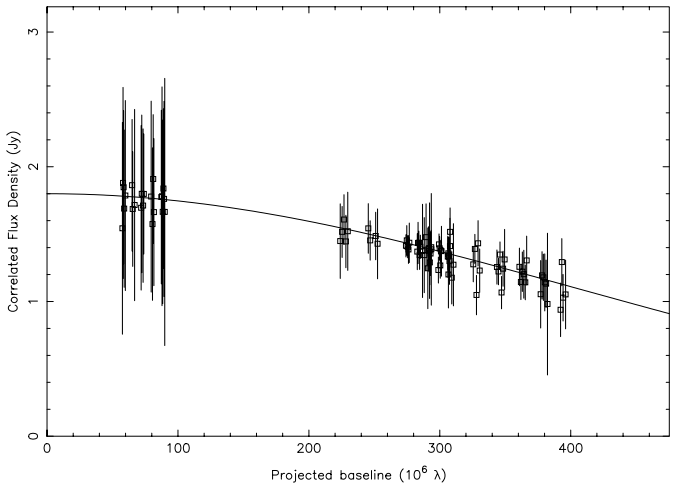


**Fig. 1.** Sgr A* at 86 GHz: correlated flux density $S_c$ (in Jy) plotted versus uv-distance (in M$\lambda$). The data were incoherently averaged to 60 sec. The solid line shows the fit of a circular Gaussian component with a flux density of 1.8 Jy and a size of 190 $\mu$as.

## 3. Data analysis and Results at 86 GHz

After the initial fringe detection of Sgr A* on single baselines with signal-to-noise ratios of up to 30 (BX: 6–16, BP: 4–6, XP: 12–30), we used the closure relations (global fringe fitting) to reduce the detection threshold and to improve the station and closure phases.

Owing to bad weather at Plateau de Bure after 06h00 UT on March 8, a closure phase for Sgr A* could be measured only during the GST interval 15h45–17h00 (5 scans). Within this time range, we find no evidence for a significant deviation of the closure phase from zero. An incoherent average of the station phases over the full scan length shows scan-to-scan variations of the closure phase of less than 10–15°. We therefore conclude that the sub-milliarcsecond structure of Sgr A* at 86 GHz must be simple, most probably point-like, or symmetric. More detailed observations are required to know if the closure phase is zero also at other hour angles.

We improved the a priori amplitude calibration by using the observed total power spectra of VX Sgr and the antenna temperatures measured in gaps between VLBI scans. Thus, we were able to correct for time dependent atmospheric opacity fluctuations. We verified the overall scaling of the amplitude calibration by comparing the visibility amplitudes of NRAO 530 with similar data obtained by B97 in April 25, 1995, close to our observations.

To determine the flux density and size of Sgr A*, we fitted a single circular Gaussian component to the visibilities (an elliptical component did not improve the fit). Probably caused by atmospheric phase and opacity fluctuations not fully corrected from observations of the calibrators, some residual 20–40 % amplitude fluctuations of the visibilities are seen between adjacent scans. To determine the effect of the remaining calibration uncertainties on the Gaussian component, we performed model fits on several data sets, which differed slightly in how they were averaged, edited, and calibrated. From this we obtained a flux density and size of the Gaussian component in the range of $S_{\rm VLBI}$ =1.5–2.2 Jy and $\theta$ = 150–220 $\mu$as, respectively. A formal error analysis based on a weighted average of these fits yields a mean flux density and size of $S_{\rm VLBI} = 1.80 \pm 0.30$ Jy and $\theta = 190 \pm 30$ $\mu$as, which we adopt as the final result. In Fig. 1 we show the data plotted versus projected baseline length together with the Gaussian component (solid line).

## 4. Data analysis at 215 GHz, Results, and Discussion

### *4.1. Fringe Fitting*

The VLBI experiment at 215 GHz was mainly aimed at the detection of compact extragalactic radio sources (see G95, K97). However, we observed also Sgr A* in three 6.5 min scans on March 2, 1995 (Table 1). Based on the results from the fringe fitting, we are confident that we have detected Sgr A* in two out of three scans:

*Detection using FRINGE (method A):* In a first analysis we used the standard program FRINGE of the correlator software for fringe detection (Rogers et al. 1983). After initial detection of $1749+096$, $1921-293$, and NRAO 530, we fringe fitted Sgr A* with single- and multi-band delay windows centered around the delays found from adjacent scans of NRAO 530 (the fringe rate window was kept fully open). We detected Sgr A* at 06h00 and 06h15 UT with an SNR of 4.6 and 6.0. The corresponding probabilities of false detection (cf. Rogers 1991) are $2.47 \cdot 10^{-5}$ and $1.74 \cdot 10^{-5}$. Detections were also obtained, when we moderately changed the sizes and the centering of the fringe search windows. The scan at 06h30 UT gave no detection (SNR=2.1, probability of false detection $1.21 \cdot 10^{-1}$).

*Detection using Incoherent Averaging (method B):* In the presence of strong atmospheric phase fluctuations and short coherence times, the fringe detection threshold can be lowered by incoherent averaging. We applied this method to the 215 GHz data, using the fringe search routines provided within the Haystack Observing Postprocessing System (HOPS, Rogers et al. 1995). For NRAO 530 and Sgr A* we incoherently averaged the coherent 6–10 sec data segments and searched for fringes in a $10 \times 10$ fringe-rate–multi-band delay grid, with the grid points spaced at the Nyquist interval. Since the incoherent fringe search is done at a fixed single band delay which is extrapolated from adjacent stronger detections, we incoherently fringed the data also at single band delays which were offset by up to $\pm 0.1 \mu$sec from the initial guess. We take the observed strong amplitude degradations at these offset positions as further evidence for the reality of the detection.

In Table 1 we summarize the results of the fringe fitting from both methods. The single- and multi-band delays (columns 3 & 4) of Sgr A* are close to each other and consistent with the corresponding values of NRAO 530, and the other sources. In good agreement with each other, methods (A) and (B) show detec-

tions of Sgr A* at 06h00 and 06h15 UT. Columns 6 (method A) and 8 (method B) summarize the corresponding signal-to-noise ratio of the fringe peaks. Note, that in method (A) a fringe peak is regarded as a significant detection, if the probability of false detection is smaller than $\sim 10^{-4}$. A similar probability cannot be calculated easily for method (B). Column 9 therefore gives the probability of misidentifying a signal with similar SNR as a fringe peak (following Rogers et al. 1995). Another estimate of the significance of a detection for method (B) comes from an empirically determined detection threshold of SNR $\geq 3$ (cf. Rogers et al. 1994, and K97).

### *4.2. Calibration and size estimate*

The size $\theta$ [$\mu$as] of a partially resolved Gaussian component with flux density $S$ [Jy] is given by:

$$\theta = 109.32 \cdot 10^3 \cdot \sqrt{\frac{-\ln C}{B^2}} \qquad (1)$$

with the compactness ratio $C = S_c/S$, and $S_c$ the correlated flux at the projected uv-spacing $B = \sqrt{u^2 + v^2}$ (in M$\lambda$). In this experiment $B = 700\,\mathrm{M}\lambda$. In the following we will discuss the flux densities $S$ and $S_c$ used in this equation.

#### 4.2.1. The flux density $S_{\rm VLBI}$ of the compact VLBI component

Unfortunately, a total flux density measurement of Sgr A* at 215 GHz is not available close to our observation in March 1995. Single dish measurements at 230 GHz gave $S_{\rm tot} = 3.3$ Jy in August 1994 (Zylka et al., 1995), and $S_{\rm tot} = 3.2$ Jy in November 1995 (Serabyn et al., 1997). These fluxes are close to each other with no indication of variability between mid 1994 and end of 1995. Using the 'quasi-simultaneous' mm/sub-mm spectra of Serabyn et al. (1997) and Falcke et al. (1998) for extrapolation to 215 GHz, we adopt a total flux density of $S_{\rm tot} = 3.1 \pm 0.1$ Jy at 215 GHz. As discussed by Serabyn et al., the observation of a mm/sub-mm excess over the $\propto \nu^{0.25}$ synchrotron power-law spectrum (solid and dashed line in Fig. 2) can be best explained by an additional structure component, perhaps extended a few ten to a few hundred mas in size. If such a component exists and is resolved by our interferometer beam, $S$ in Eq. (1) should be replaced with a flux density corrected for the contribution of this additional component $S_{\rm VLBI} = S_{\rm tot} - S_{\rm ext}$. In order to separate the total flux of the compact VLBI component $S_{\rm VLBI}$ from the total flux $S_{\rm tot}$ at 215 GHz, we extrapolate the flux density $S_{\rm VLBI}$ from the available spectral data of the VLBI core at lower frequencies (dashed line in Fig. 2). We note that the differences between the mean spectra of the VLBI component at earlier dates (an arbitrary binning of 1974–1977, 1982–1985 and 1991–1995 was chosen) indicates long term variability of Sgr A* (cf. Zylka et al., 1995, Mezger et al., 1996). With the spectrum located nearest in time to the epoch of the total spectrum (1996), we obtain $S_{\rm VLBI} = 2.0 \pm 0.2$ Jy at 215 GHz. The flux density excess of $S_{\rm ext} = S_{\rm tot} - S_{\rm VLBI} = 1.10 \pm 0.2$ Jy thus could be attributed to the additional contribution from a component so far undetected by mm-VLBI.

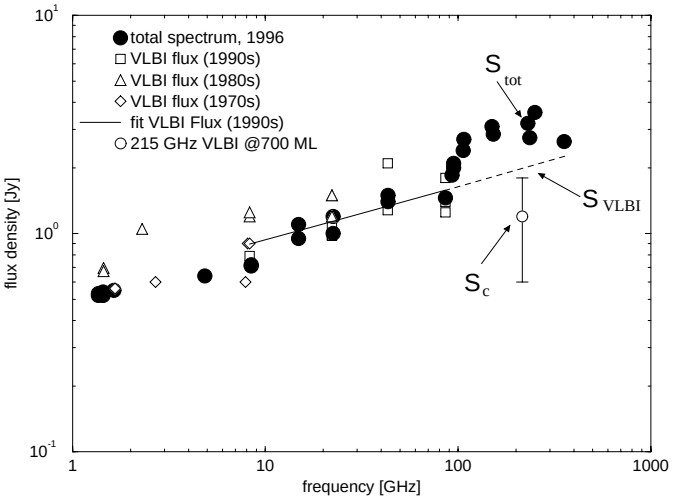


**Fig. 2.** The cm- to mm-spectrum of Sgr A*. Filled circles show the total flux $S_{\rm tot}$ from Serabyn et al. 1997 and Falcke et al. 1998. Open symbols denote fluxes of the VLBI component ($S_{\rm VLBI}$) at 3 arbitrarily binned time intervals: open squares for the 1990s, open triangles for the 1980s, open diamonds for the 1970s. The solid line shows a power-law fit to the VLBI spectrum of the 1990s ($S_{\rm VLBI}[\mathrm{Jy}] = 0.535 \cdot \nu^{+0.24}_{\rm GHz}$), which compares well with the total spectrum (filled circles). Above $\nu > 100$ GHz the difference between total flux and extrapolated spectrum (dashed line) indicates a flux density excess. At 215 GHz a correlated flux of $S_c = 1.2 \pm 0.6$ Jy ($B = 700\,\mathrm{M}\lambda$) has been measured (open circle).

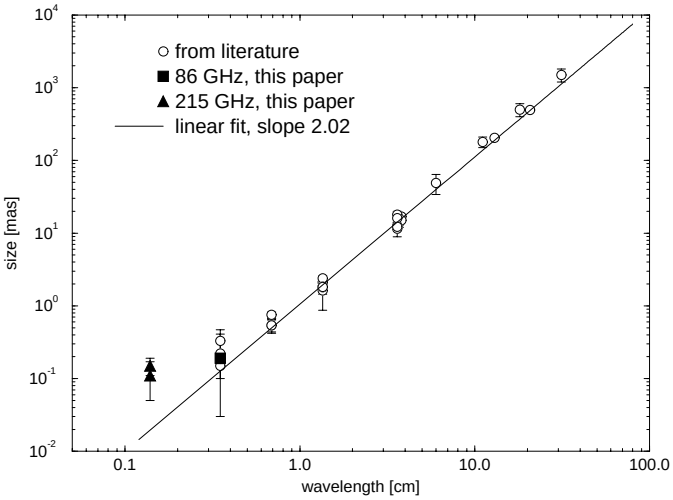


**Fig. 3.** The size of Sgr A* plotted versus wavelength. The solid line shows a fit to the data, excluding the data points at 1.4 mm wavelength. A filled square denotes our measurement at 86 GHz ($190 \pm 30\,\mu$as), filled triangles at 215 GHz ($\theta_1 = 150 \pm 40\,\mu$as, respectively $\theta_2 = 110 \pm 60\,\mu$as, see text).

#### 4.2.2. The correlated flux density $S_c$

The 215 GHz VLBI data were calibrated as described in G95 & K97. As outlined in these papers, the calibration at 215 GHz is

**Table 1.** Observation of Sgr A* at 215 GHz on March 2, 1995. The columns give (1) start time of the scan, (2) source name, (3) single-band delay, (4) multi-band delay, (5) fringe rate, (6) signal-to-noise ratio after average over the full scan lengths using FRINGE, (7) probability of false detection (FRINGE), (8) signal-to-noise ratio after incoherent averaging (HOPS), (9) probability of misidentifying this signal, and (10) a statement on the quality of the detection.

| Time UT | Source | SBD $\mu$sec | MBD $\mu$sec | FR psec/sec | SNR | PFD | $\mathrm{SNR_{inc}}$ | PID | Detection at 215 GHz |
|---|---|---|---|---|---|---|---|---|---|
| 05h15 | NRAO 530 | 0.009 | 0.026 | 0.07 | 5.4 | $8.81 \cdot 10^{-5}$ | 4.6 | $1.71 \cdot 10^{-9}$ | yes |
| 05h30 | NRAO 530 | −0.015 | 0.028 | 0.03 | 7.2 | $3.23 \cdot 10^{-11}$ | 5.5 | $1.11 \cdot 10^{-14}$ | yes |
| 05h45 | NRAO 530 | −0.002 | 0.027 | 0.03 | 2.6 | $3.75 \cdot 10^{-2}$ | 4.5 | $5.55 \cdot 10^{-9}$ | marginal |
| 06h00 | Sgr A* | −0.010 | 0.038 | −0.08 | 4.6 | $2.47 \cdot 10^{-5}$ | 2.9 | $7.30 \cdot 10^{-3}$ | marginal |
| 06h15 | Sgr A* | −0.006 | 0.035 | −0.03 | 6.0 | $1.74 \cdot 10^{-5}$ | 4.9 | $4.02 \cdot 10^{-11}$ | yes |
| 06h30 | Sgr A* | −0.003 | 0.050 | −0.30 | 2.1 | $1.21 \cdot 10^{-1}$ | 2.1 | $3.68 \cdot 10^{-1}$ | no |
| 06h45 | NRAO 530 | −0.004 | 0.029 | 0.05 | 11.7 | $2.09 \cdot 10^{-29}$ | 11.7 | 0 | yes |
| 07h00 | NRAO 530 | −0.008 | 0.028 | 0.08 | 8.6 | $8.00 \cdot 10^{-16}$ | 10.8 | 0 | yes |
| 07h15 | NRAO 530 | −0.004 | 0.026 | 0.11 | 2.5 | $4.71 \cdot 10^{-2}$ | 2.5 | $6.92 \cdot 10^{-2}$ | no |

less accurate than at 86 GHz, and–for all 8 sources detected at 215 GHz–resulted in relatively low correlated flux densities with compactness ratios $C = 12$–$38\,\%$ (K97). Probably the main source for systematic calibration errors are inaccurately known system temperatures and atmospheric opacities at low elevations. Phase stability tests performed with the VLBI equipment (G95, K97) and the phase coherence of the data ($\leq 20\,\%$ amplitude losses within $6-8$ sec coherence time) exclude a strong amplitude degradation by phase fluctuations. The analysis of systematic calibration errors therefore leaves room for a calibration uncertainty, which would increase the correlated flux by not more than a factor of 1.5–2 (see also K97). Larger factors would lead to system equivalent flux densities (SEFD) at both stations which are rather implausible[1]. We reject this possibility since the correlated flux densities of 3C279, 1749+096, NRAO 530, 1921−293 (see K97) would come out too large, partly exceeding their single dish flux densities. The 'a priori' calibration gives a correlated flux density for Sgr A* of $S_c = 0.6$–$0.8$ Jy ($B = 700\,\mathrm{M}\lambda$). With the flux density scale possibly being low by a factor of $\leq 2$, an upper limit for the correlated flux of $S_c \leq 1.6$ Jy is obtained. With regard to this uncertainty we therefore adopt for the following $S_c = 1.2 \pm 0.6$ Jy (open circle in Fig. 2), which covers the possible range of $S_c$ including calibration errors.

#### 4.2.3. The source size

As explained above, the source size depends on the exact value of the total flux of the VLBI component. *Without* the extended component postulated from the mm/sub-mm excess, we obtain from Eq. (1) and setting $S = S_{\mathrm{tot}} = 3.1 \pm 0.1$ Jy a size of $\theta_1 = 150 \pm 40\,\mu$as (case 1). If on the other hand an additional structure component exists, we must use $S = S_{\mathrm{VLBI}} = S_{\mathrm{tot}} - S_{\mathrm{ext}} = 2.0 \pm 0.2$ Jy, which yields a size of $\theta_2 = 110 \pm 60\,\mu$as (case 2). The formal error in these numbers mainly comes from the uncertainty of $S_c$. For the most extreme case of a calibration low by a factor 2, a lower limit to the source size of $\theta_2 \geq 50\,\mu$as is obtained (note: this becomes smaller if the calibration uncertainty would be $\geq 2$).

In Fig. 3, we plot the size of Sgr A* versus wavelength, adding our results to the data from the literature (Krichbaum et al. 1994, Yusef-Zadeh et al. 1994, B97, and references therein). A power law fit (excluding the 1.4 mm data) gives a slope of $a = 2.02 \pm 0.01$ ($\theta \propto \lambda^a$), very close to $a = 2$ expected for scatter broadening. We determine from the fit a scattering size of $135 \pm 5\mu$as at 86 GHz and $20 \pm 5\mu$as at 215 GHz. While the observed source size at 86 GHz is only marginally larger than the scattering size ($\theta = 190 \pm 30\,\mu$as this paper; $\theta = 150 \pm 50\,\mu$as from Rogers et al., 1994), the sizes measured at 215 GHz seem to be much larger than the scattering size. Obviously $\theta_2$ agrees better with the expected $20\,\mu$as size, than $\theta_1$. This supports the hypothesis of additional source structure, that is either completely resolved by VLBI, or at least not seen in this snap-shot observation.

If Sgr A* is assumed to be a homogeneous synchrotron self-absorbed source with a brightness temperature at 215 GHz near $T_B \simeq (1-2) \cdot 10^{10}$ K (as extrapolated from $\nu \leq 86$ GHz), a magnetic field of $B \simeq 30-60$ G can be derived. At 215 GHz, the expected size then would be $\theta = 70$–$90\,\mu$as. This corresponds to 11–14 Schwarzschild radii ($\mathrm{R}_s$) for a $2.6 \cdot 10^6\,\mathrm{M}_\odot$ black hole, which is in agreement with our size estimate ($\theta_2 = 17 \pm 9\,\mathrm{R}_s$).

## 5. Summary

At 86 GHz, the VLBI structure of Sgr A* is symmetric (zero closure phase) and can be described by a circular Gaussian component with flux density $S_{\mathrm{VLBI}} = 1.80 \pm 0.30$ Jy, and size $\theta = 190 \pm 30\,\mu$as, close to the expected scattering size of 135 $\mu$as. At 215 GHz, Sgr A* was marginally detected on the 1150 km baseline between Pico Veleta and Plateau de Bure. Depending on the nature of the mm/sub-mm flux density excess and remaining calibration uncertainties, the source size at 215 GHz lies in the range of $50 \leq \theta \leq 190\,\mu$as, probably larger than the scattering size of $20\mu$as. Based on the brightness temperature and total flux of Sgr A* extrapolated from lower frequencies,

[1] The correlated flux is proportional to the geometric mean of the SEFD's of both stations.

our best size estimate at 215 GHz is $\theta = 110 \pm 60\,\mu$as, or $17 \pm 9$ Schwarzschild radii (M$= 2.6 \cdot 10^6$ M$_\odot$ ). A size smaller than this cannot yet definitively be ruled out, but would imply unreasonable large calibration errors. A hard lower limit to the source size is set by the Schwarzschild diameter of $13\mu$as for the above black hole, which becomes equal to the scattering size near 270 GHz. Thus, future 1 mm VLBI observations with intercontinental baselines ($20 - 30\,\mu$as fringe spacing) should determine how compact Sgr A* really is.

*Acknowledgements.* We thank the staff of the observatories and A. Barcia, I. López–Fernández (Yebes) and M. Torres (IRAM) for their efficient support. We thank CNRS-INSU France for providing the Hydrogen Maser, and the Yebes observatory for the terminal for Plateau de Bure. For their contributions and discussion we thank S. Doeleman, H. Falcke, A. Lobanov, H. Matsuo, P. Mezger, I. Pauliny-Toth, A. Rogers, E. Serabyn, and R. Zylka.

## References

Backer D.C., Zensus J.A., Kellermann K.I., et al., 1993, Sci, 262, 1414.
Bower G.C., Backer D.C., Wright M.C.H., et al., 1997, ApJ, 484, 118 (B97).
Falcke H., Goss W.M., Matsuo H., et al. 1998, ApJ, in press.
Genzel R., Eckart A., Ott T., Eisenhauer F., 1997, MNRAS, 291, 219.
Greve A., Torres M., Wink J.E., et al., 1995, A&A, 299, L33 (G95).
Krichbaum T.P., Zensus J.A, Witzel A., et al., 1993, A&A, 274, L37.
Krichbaum T.P., Schalinski C.J., Witzel A., et al., 1994, in: The Nuclei of Normal Galaxies: Lessons from the Galactic Center, ed. R. Genzel and A.I. Harris, ASI Conference Series C, Vol. 445, (Kluwer, Dordrecht), p. 411.
Krichbaum T.P., Graham D.A., Greve A., et al., 1997, A&A, 232, L17 (K97).
Mezger P.G., Duschl W.J., and Zylka R., 1996, A&AR, 7, 289.
Rogers A.E.E., Capallo R.J., Hinteregger H.F., et al., 1983, Sci, 219, 51.
Rogers A.E.E., 1991, in: Frontiers of VLBI, Frontiers Science Series No. 1, ed. H. Hirabayashi, M. Inoue and K. Kobayashi (Universal Academy Press, Tokyo), p. 341.
Rogers A.E.E., Doeleman S., Wright M.C.H., et al., 1994, ApJ, 434, L59.
Rogers A.E.E., Doeleman S.S., and Moran J.M., 1995, AJ, 109, 1391.
Serabyn E., Carlstrom J., Lay O., et al., 1997, ApJ, 490, L77.
Yusef-Zadeh F., Cotton W., Wardle M., Melia F., and Roberts D.A., 1994, ApJ, 434, L63.
Zylka R., Mezger P.G., Ward-Thompson D., Duschl W.J., and Lesch H., 1995, A&A, 297, 83.